Electronic Supplementary Material (ESI) for Materials Chemistry Frontiers.

Supporting Information

Rational design and facile preparation of maleimide-based functional materials for imaging and optoelectronic applications

Ze Yang,[a‡] Yun Guo,[a‡] Shu-Lun Ai,[a] Su-Xiao Wang,[a] Jin-Zhi Zhang,[a*] Yue-Xing Zhang,[a*] Qi-Chao Zou[a] and Hang-Xing Wang[a*]

[a] Key Laboratory for the Synthesis and Application of Organic Functional Molecules (MOE), College of Chemistry and Chemical Engineering, Hubei University, Wuhan, 430062, P.R. China.

Email: zjz4000@126.com; zhangyuexing@hubu.edu.cn; wanghx0917@163.com

Experimental Procedures

1. Materials

All reagents as received from commercial sources were used after re-crystallization, and all solvents were used after distillation process. All experiments were carried out under air atmosphere. Reagent grades of L-tartaric acid (TA), (+)-diacetyl-L-tartaric anhydride were purchased from Energy-Chemical (Shanghai, China) and the rest of the amines were purchased from commercial sources. The deionized (DI) water was used throughout this study. Column chromatographic purifications were carried out on flash silica-gel (240–400 mesh) using petroleum ether (PE) and ethyl acetate (EA) as eluents.

2. Characterizations

^{1}H and ^{13}C NMR spectra were obtained on a Bruker AV-600 MHz spectrometer. Mass spectra were taken on LC-MS (ESI) mass spectrometer. UV/Vis absorption spectra were recorded with a T6 UV/Vis Spectrometer. The photoluminescence (PL) spectra were performed using a LS55 Fluorescence Spectrometer (PerkinElmer, USA). Photographs of PL were taken using a Canon camera (EOS 550) under excitation by a hand-hold UV lamp (365 nm). The absolute fluorescence quantum yields were measured using a FLS980 system. Cellular imaging was performed with a confocal laser fluorescence microscopy (TCS SP5II, Leica, Germany). The cyclic voltammetry curves were measured with an electrochemical analyzer (660B, CHI Instruments). Electrochemical impedance spectroscopy (EIS) Nyquist plot obtained at an AC

voltage with amplitude of 5 mV over the frequency range of 1×10^{-3} to 1×10^{5} Hz for electrodes in tetrabutyl ammonium fluoride/acetonitrile (0.1 mol/L).

3. Computational details

The molecular structures of BPD and BBPD were fully optimized with B3LYP functional and 6-31G(d) basis set in chloroform solvent with using the CPCM polarizable conductor calculation model using Gaussian 16 software.[1] Harmonic-model vibrational frequencies were calculated based on the optimized geometries to verify the optimized structure to be true energy minimum. UV-vis spectroscopic calculations were made by a time-dependent (TD)-DFT method with the same method as ground state optimization based on the optimized geometry. The geometry of the first excited state was also optimized with TDDFT method to study the emission behavior.

4. The in vitro cytotoxicity study

The cell viability was evaluated on human cervical cancer (Hela) cells using a standard 3-(4, 5-dimethylthiazol-2-yl)-2, 5-diphenyltetrazolium bromide (MTT) assay.[2] Typically, cells were seeded in 96-well culture plates and allowed to grow over 24 h at 37 ^{o}C. After the incubation, the culture medium was discarded and then cells were treated with Dulbecco's Modified Eagle's Medium (DMEM), containing various concentrations (0-500 μg/mL) of the aminomaleimides (BBPD and BMPD) for another 24 h. At the end of the incubation, the culture medium was removed, and

20 μL of MTT (5.0 mg/mL in PBS) was added into each well. After additional 4 h incubation, the growth medium was removed and 200 μL of dimethyl sulfoxide (DMSO) was added. Finally, optical density of each sample was recorded using a microplate reader (Imark 168-1130, Biorad, USA) at a wavelength of 405 nm. The cells treated with phosphate buffer solution (PBS) and DMSO, which did not contain aminomaleimides, were taken as the control group and six parallel samples were tested in each group. The cell viability was calculated based on the following equation:

Cell viability = $OD_{treated}$ / $OD_{control}$ X 100%,

where $OD_{treated}$ was obtained from the cells treated by the samples and the $OD_{control}$ was obtained from the untreated cells.

5. Fluorescence imaging

The potential for bioimaging of 1-butyl-3-(2-methoxy-2-oxo-1-amino)-1H-pyrrole-2,5-dione (BMPD) was tested using HeLa cells as similar to our previous work.[3] The potential for cellular imaging of the as obtained BMPD was tested by the use of HeLa cells. Typically, 2.0 mL of HeLa cells in DMEM medium at an initial density of 4×10^4 cell per mL were seeded in each dish and cultured at 37°C for 24 h under a humidified atmosphere containing 5% CO_2. The dispersion of the BMPD was prepared in DMEM medium with a concentration of 248 μg/mL. Cells were cultured with the dispersion of BMPD for 4 h and then washed three times with PBS to

remove the free BMPD. Finally, the samples were observed with confocal laser fluorescence microscopy.

6. Photocurrent performance measurement

A photoelectrochemical (PEC) cell with three-electrode configuration was constructed as similar to our previous work.[4] The platinum wire and saturated calomel electrode (SCE) were respectively used as the counter electrode and the reference electrode. The PEC performance of the photoelectrode was measure in 0.1 M tetrabutyl ammonium fluoride/acetonitrile electrolyte. A 300 W Xe lamp was used as light source. The current response was recorded with a CHI 660B electrochemical workstation. The photocurrent response activities of the BPD and BBPD solutions subjected to light on/off cycles were measured.

7. Etched ITO electrode and device

The ITO area used as electrodes was protected by tapes with adhesive tape exposed, and then the tape-protected ITO was coated with a layer of zinc powder and immersed into 1 M hydrochloride solution to etch ITO without tape protection.[5] Second, the BBPD crystal sample was coated onto the etched area to link the two electrodes, and the joints were covered with conductive silver glue.

8. Preparation of GFGA-based solar cell

The solar cell device was fabricated with a sandwiches structure by assembling the ITO photoanode and carbon electrode photocathode. The graphite-based photocathode was prepared by adopting a 2H pencil to coat the graphite on the frosted glass by friction. The gel-state GFGA was firstly transferred to the ITO substrate, and then the graphite/glass substrate was directly covered the GFGA layer. The effective area of the device is ca. 0.5 cm^2.

Synthesis

1. Synthesis of 1-butyl-1H-pyrrole-2, 5-dione (BPD)

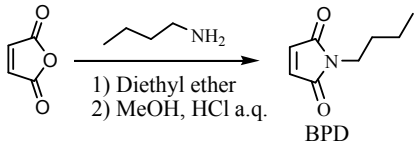

The target BPD is designed and synthesized as according to pervious report.[6] In a typical procedure, n-butylamine (4.50 g, 61.5 mmol) dissolved in 10 mL of diethyl ether was added to maleic anhydride (6.10 g, 62.2 mmol) in 150 mL diethyl ether. The system was stirring at 0 ^{o}C for 3 h, a white powder of N-substituted maleamic acid was recovered by filtration. After a solution containing N-substituted maleamic acid and methanol/conc. HCl (5:1, 30 mL) was heated at reflux for 16 h. The MeOH was removed under reduced pressure and the aqueous residue extracted with ethyl acetate (3×20 mL). The organic extracts were dried over Na_2SO_4 and concentrated under reduced pressure. The crude residue was purified by flash chromatography (PE/EA, v/v=14:1) to obtain BPD (30.2 %). ^{1}H NMR (600MHz, $CDCl_3$) δ(ppm): 6.67 (s, 2 H), 3.50 (t, 2 H), 1.58–1.52 (m, 2 H), 1.31–1.27 (m, 2 H), 0.92 (t, 3 H). ^{13}C NMR (600MHz, $CDCl_3$) δ(ppm): 170.9, 134.0, 37.6, 30.6, 19.9, 13.5.

2. Synthesis of 1-butyl-3, 4-dihydroxy-(3R, 4R)-5-pyrrolidinedione (BDPD)

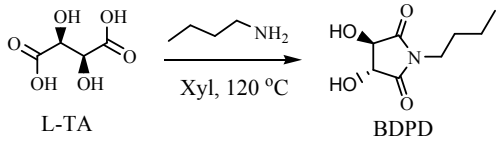

The target BDPD is synthesized through amidation reaction.[7] In a typical procedure, n-butylamine (321.8 mg, 4.4 mmol) dissolved in 3 mL of xylenes added to L-tartaric

acid (600.4 mg, 4.0 mmol) in 12 mL xylenes was stirred at 120 °C for 2 h, the reaction mixture was then cooled to room temperature and filtered, and then the solid was recrystallized in water to obtain BDPD (45.1 %). ^{1}H NMR (600MHz, $(CD_3)_2SO$) δ(ppm): 6.21 (s, 2 H), 4.29 (s, 2 H), 3.40–3.30 (m, 2 H), 1.48–1.42 (m, 2 H), 1.26–1.18 (m, 2 H), 0.87-0.84 (t, 3 H). ^{13}C NMR (600 MHz, $(CD_3)_2SO$) δ(ppm): 174.75, 74.40, 37.43, 29.21, 19.43, 13.49.

3. Synthesis of 1-butyl-3-(butylamino)-1H-pyrrole-2, 5-dione (BBPD)

Route 1

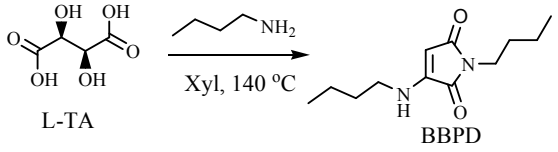

In a typical process, n-butylamine (614.4 mg, 8.4 mmol) dissolved in 3 mL of xylenes was added to L-tartaric acid (600.4 mg, 4.0 mmol) in 12 mL xylenes. The reaction mixture was stirred at 150 °C for 5 h and then cooled to room temperature and filtered. The solvent was removed under reduced pressure, and the crude residue was purified by flash chromatography (PE:EA, v/v=10:1) to afford BBPD as a yellowish solid powder in 8.1 % yield. ^{1}H NMR (600MHz, $CDCl_3$) δ(ppm): 5.34 (s, 1 H), 4.77 (s, 1 H), 3.47–3.44 (t, 2 H), 3.18–3.14 (m, 2 H), 1.63–1.60 (m, 2 H), 1.56–1.53 (m, 2 H), 1.42–1.39 (m, 2 H), 1.31-1.30 (m, 2 H), 0.96-0.94 (t, 3 H), 0.93-0.90 (t, 3 H). ^{13}C NMR (600 MHz, $CDCl_3$) δ(ppm): 212.99, 206.61, 196.05, 195.81, 189.27, 182.62, 149.86, 149.61, 149.27, 142.83, 58.99, 53.91.

Route 2

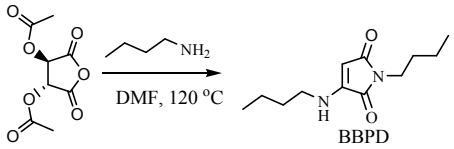

In a typical process, n-butylamine (307.0 mg, 4.2 mmol) dissolved in 10 mL of dimethyl formamide (DMF) was added to (+)-diacetyl-L-tartaric anhydride (216.0 mg, 1.0 mmol) in 20 mL DMF. The reaction mixture was stirred at 120 °C for 5 h and then cooled to room temperature and filtered. The solvent was removed under reduced pressure, and the crude residue was purified by flash chromatography (PE:EA, v:v=10:1) to afford BBPD as a yellowish solid powder in 20.5 % yield.

4. Synthesis of 1-butyl-3-(2-methoxy-2-oxo-1-amino)-1H-pyrrole-2, 5-dione (BMPD)

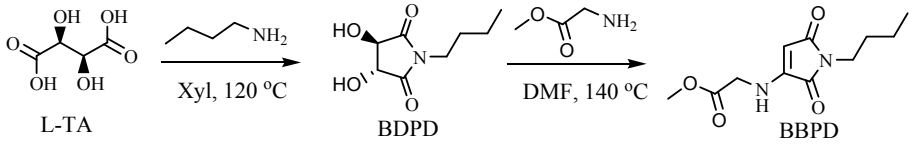

In a typical process, BDPD (374.2 mg, 2 mmol) and methyl glycinate (391.8, 4.4 mmol) in 15 mL of DMF was stirred at 140 °C for 4 h, the reaction mixture was then cooled to room temperature and filtered, and then the solvent was removed under reduced pressure. The crude residue was purified by flash chromatography (PE:EA, 1:1) to obtain BMPD (20.1 %). ^{1}H NMR (600MHz, $CDCl_3$) δ(ppm): 5.78 (s, 1 H), 4.83 (s, 1 H), 3.92–3.91 (t, 2 H), 3.82 (s, 3 H), 3.48–3.45 (t, 2 H), 1.57-1.53 (m, 2 H), 1.34-1.27 (m, 2 H), 0.93-0.90 (t, 3 H). ^{13}C NMR (600 MHz, $CDCl_3$) δ(ppm): 197.79, 191.45, 185.02, 180.82, 173.74, 166.54, 134.59, 134.33, 134.07, 40.50, 38.18.

5. Preparation of GFGA

The GFGA was prepared by direct heating treatment of the aqueous mixture of L-tartaric acid + n-butylamine at 120 ^{o}C in a round-bottom flask. In a typical procedure, L-tartaric acid (4.50 g, 30.0 mmol) was added into a round-bottom flask and then completely dispersed in H_2O (10 mL). The n-butylamine (8.76 g, 120.0 mmol) was added showly into the L-tartaric acid aqueous using a constant pressure funnel. The round-bottom flask was placed in an ice bath and stirred for 4 h. Following, heating treatment of the aqueous mixture of L-tartaric acid + n-butylamine at 120 ^{o}C for another 24 h. The sample was changed from colorless liquid to transparent gel-like product, indicating the formation of GFGA.

Tables, Figures and Schemes

Table S1 Absorption and emission properties of BBPD in selected solvents.

Solvent	ET(30)[a]	λ_{abs} (nm)	λ_{em} (nm)	QY(%)[b]
Hexane (Hex)	31.0	241/345	456	94.6
Tetrahydrofuran (THF)	37.4	258/358	478	73.9
Dichloromethane (DCM)	40.7	244/361	478	42.5
Acetonitrile (MeCN)	45.6	244/360	480	41.5
Methanol (MeOH)	55.4	242/368	510	2.1

[a] The microscopie solvent polarity parameter.[8] [b] The absolute fluorescent quantum yields (QYs) of the BBPD are determined in an integrating sphere by using an absolute method.

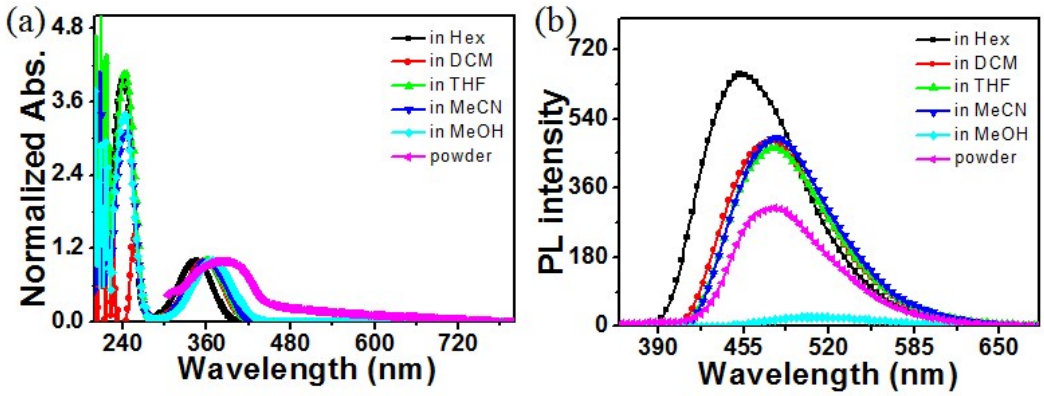

Figure S1. (a) Normalized UV/Vis spectra of BBPD in various solvents including Hex, DCM, THF, MeCN, MeOH, and solid film. (b) PL spectra of BBPD solution and solid film.

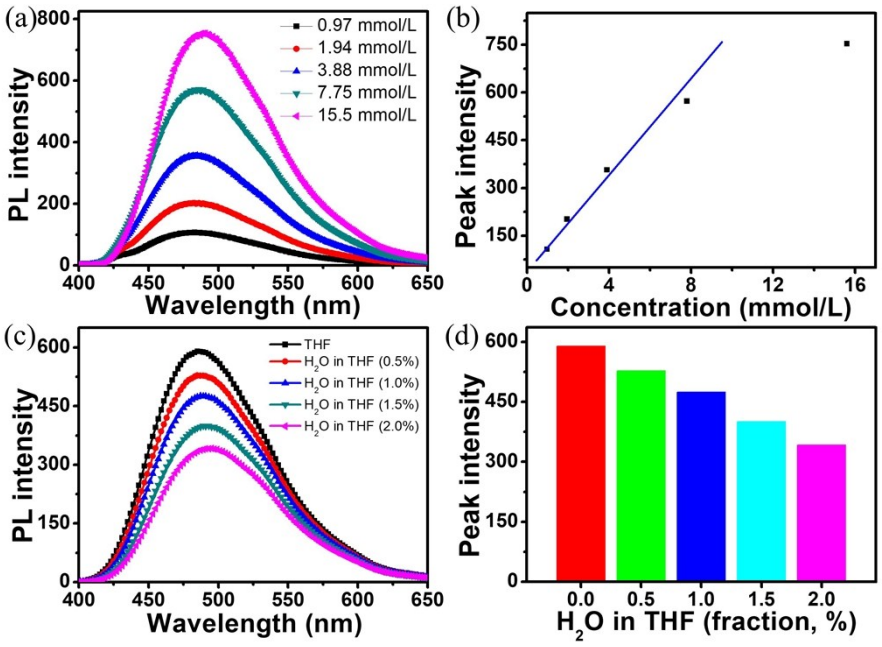

Figure S2. (a) PL spectra of BBPD in DCM with different concentration from 0.97 to 15.5 mmol/L and (b) the calibration curve. (c) PL spectra of BBPD in THF with different fraction of H_2O and (d) the histogram of fluorescence intensity.

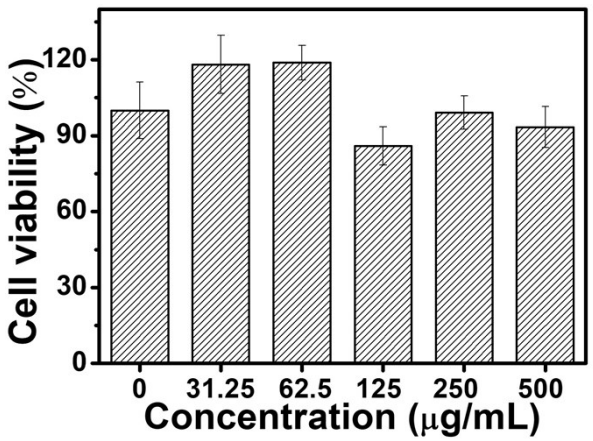

Figure S3. Cytotoxicity assessment: viability of HeLa cells incubated with the BBPD (31.25-500 μg/mL) and MTT (20 μL, 5 mg/mL).

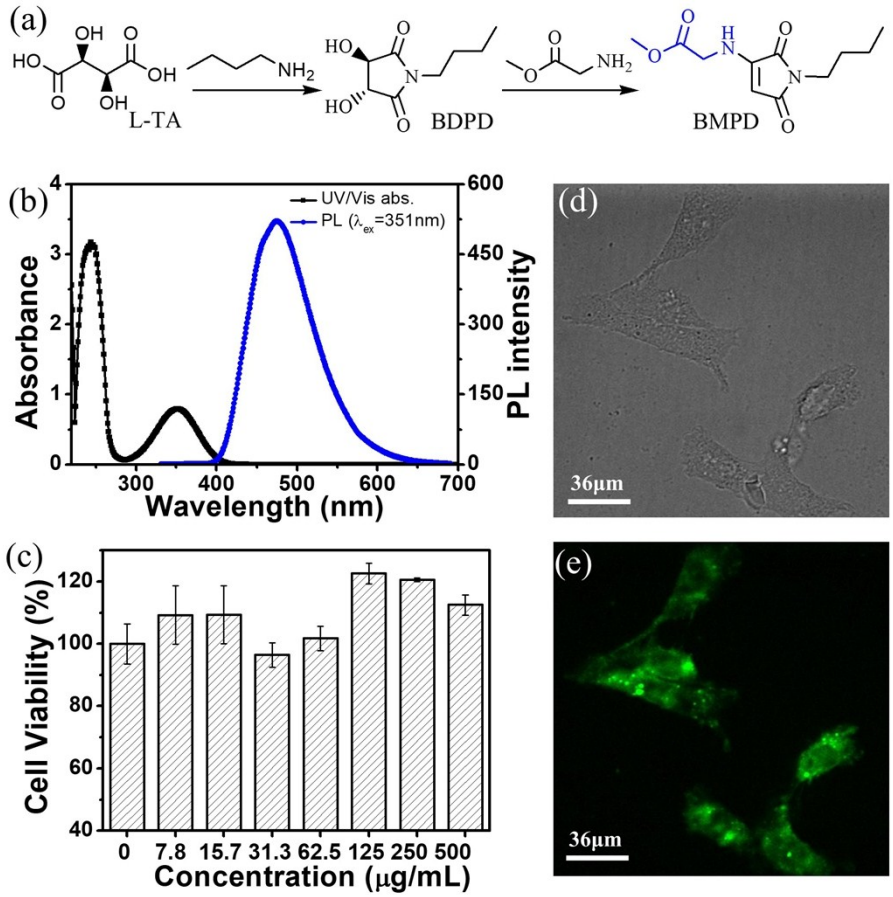

Figure S4. (a) Synthetic route toward BMPD. (b) UV/Vis and PL spectra of BMPD in DCM. (c) Cytotoxicity assessment: viability of HeLa cells incubated with the BMPD (7.8-500 μg/mL) and MTT (20 μL, 5 mg/mL). (d-e) Confocal fluorescence images of HeLa cells incubated with 200 μg/mL of BMPD for 4 h. The scale-bar is 36 μm.

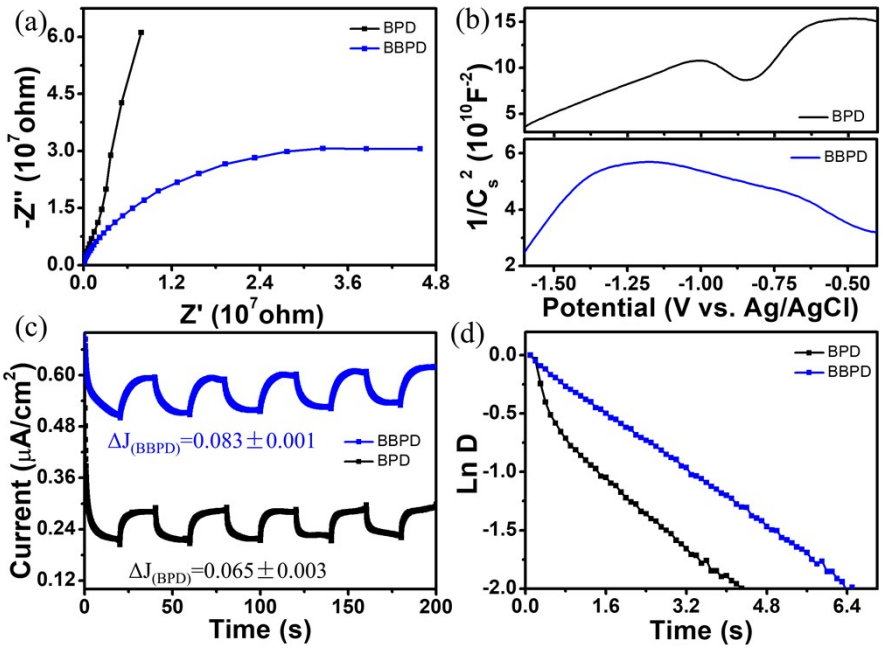

Figure S5. (a) EIS Nyquist plots of the BPD and BBPD. (b) Periodic on−off current-time curves of the BPD and BBPD photoeletrodes. (c) Normalized plots of the photocurrent-time dependence for the BPD and BBPD. (d) Mott–Schottky plots of the BPD and BBPD in 0.005 M $[Fe(CN)_6]^{3-/4-}$ solution in 0.1 M KCl solution under dark condition.[9]

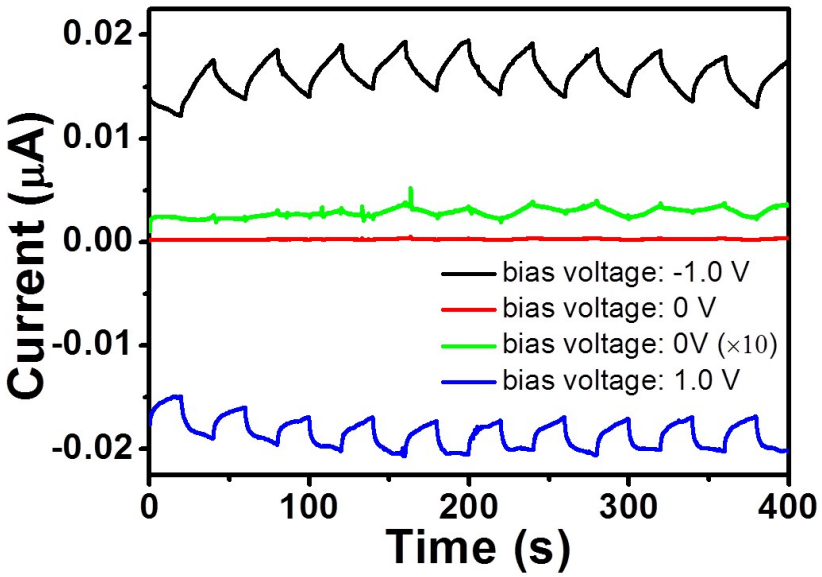

Figure S6. The plots of photocurrent response of the BBPD crystal on the etched ITO substrate under different bias voltages.

Table S2 Crystal data and structure refinement parameters for BBPD.

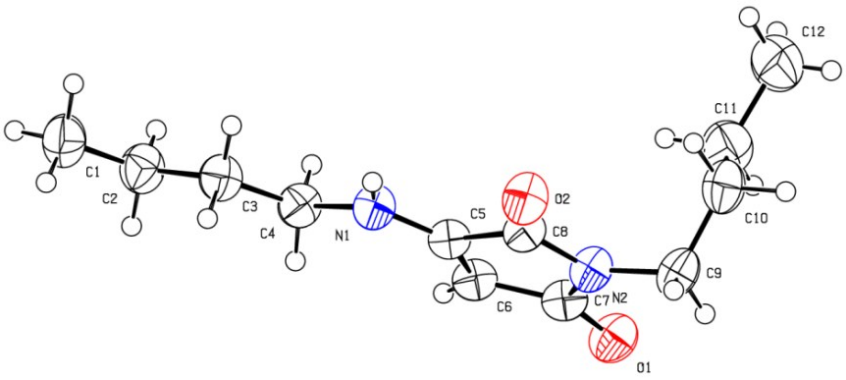

Bond precision: C-C = 0.0037 A		Wavelength = 1.54184
Cell: a = 4.9828(6) b = 9.8944(5) c = 13.3739(11)		
alpha = 97.868(6) beta = 91.376(8) gamma = 102.696(8)		
Temperature: 195 K		
	Calculated	Reported
Volume	636.18(10)	636.18(10)
Space group	P -1	P -1
Hall group	-P 1	-P 1
Moiety formula	$C_{12}H_{20}N_2O_2$	$C_{12}H_{20}N_2O_2$
Sum formula	$C_{12}H_{20}N_2O_2$	$C_{12}H_{20}N_2O_2$
Mr	224.30	224.30
Dx, g cm^{-3}	1.171	1.171
Z	2	2
Mu (mm^{-1})	0.643	0.643
F000	240	240
F000'	244.71	
h, k, l_{max}	5,11,16	5,11,16
N_{ref}	2281	2263
T_{min}, T_{max}	0.926, 0.950	0.837, 1.000
$T_{min'}$	0.908	
Correction method = # Reported T Limits: T_{min}=0.837 T_{max}=1.000		
AbsCorr = MULTI-SCAN		
Data completeness = 0.992		Theta(max) = 67.480
R(reflections) = 0.0649(1905)		wR2(reflections) = 0.2174(2263)
S = 1.087		Npar = 226

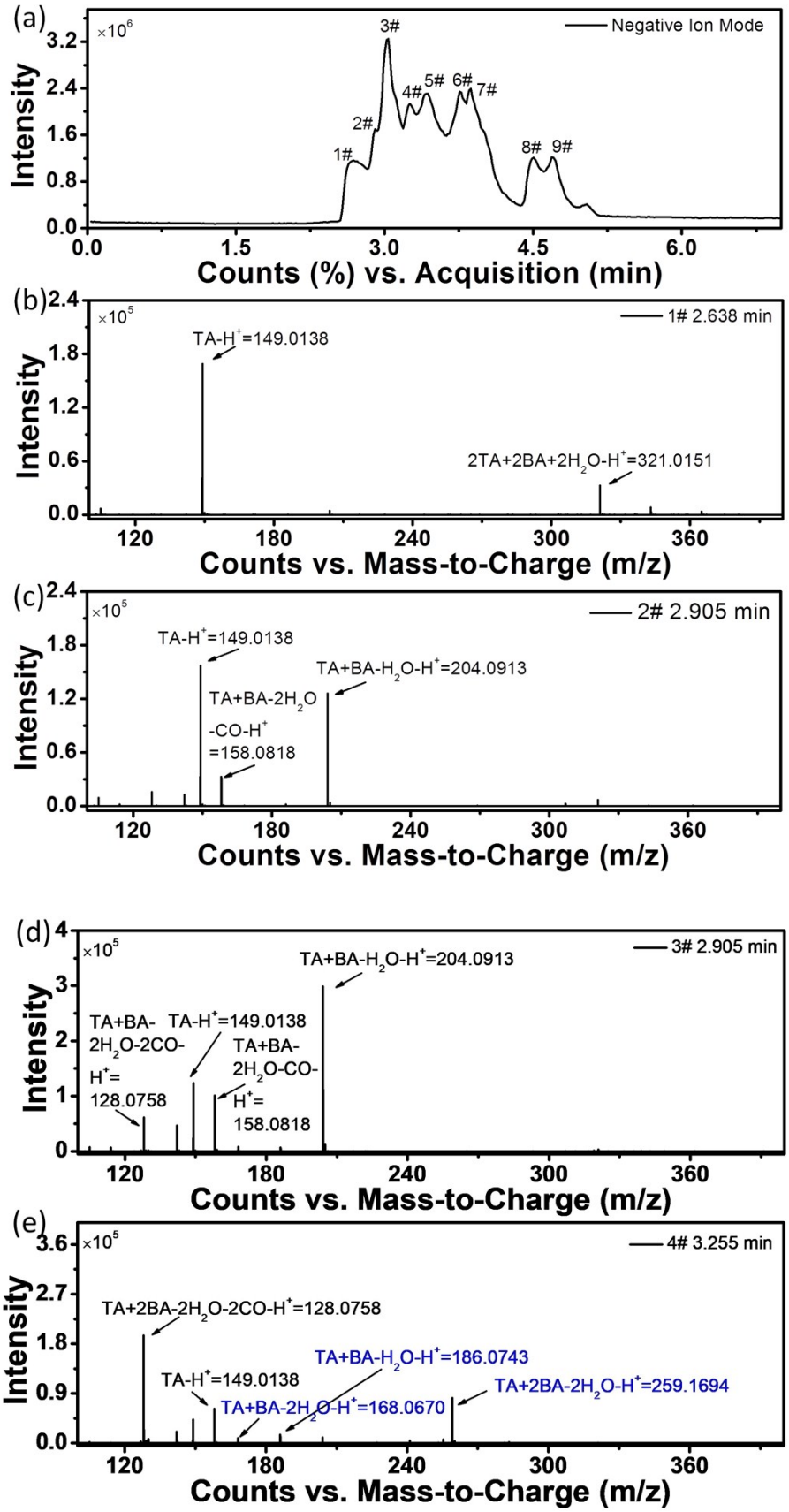
(a)
×10^6
Negative Ion Mode
3#
2#
1#
4#
5#
6#
7#
8#
9#
Intensity
Counts (%) vs. Acquisition (min)
(b)
×10^5
1# 2.638 min
TA-H+=149.0138
2TA+2BA+2H2O-H+=321.0151
Intensity
Counts vs. Mass-to-Charge (m/z)
(c)
×10^5
2# 2.905 min
TA-H+=149.0138
TA+BA-H2O-H+=204.0913
TA+BA-2H2O -CO-H+ =158.0818
Intensity
Counts vs. Mass-to-Charge (m/z)
(d)
×10^5
3# 2.905 min
TA+BA-H2O-H+=204.0913
TA+BA-2H2O-2CO-H+= 128.0758
TA-H+=149.0138
TA+BA-2H2O-CO-H+= 158.0818
Intensity
Counts vs. Mass-to-Charge (m/z)
(e)
×10^5
4# 3.255 min
TA+2BA-2H2O-2CO-H+=128.0758
TA+BA-H2O-H+=186.0743
TA-H+=149.0138
TA+BA-2H2O-H+=168.0670
TA+2BA-2H2O-H+=259.1694
Intensity
Counts vs. Mass-to-Charge (m/z)

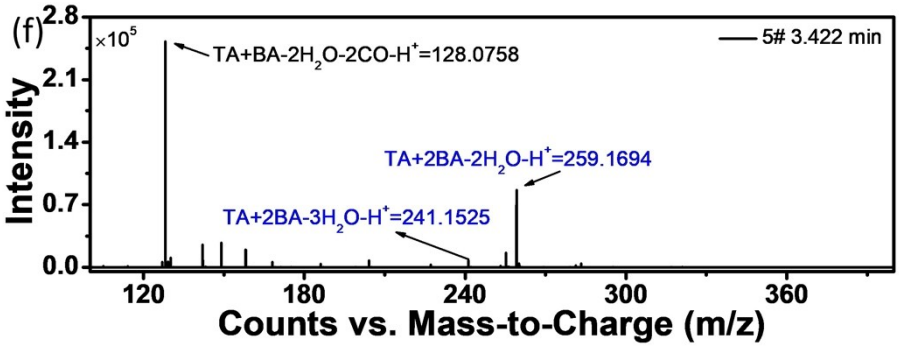
(f)
×10^5
5# 3.422 min
TA+BA-2H2O-2CO-H+=128.0758
TA+2BA-2H2O-H+=259.1694
TA+2BA-3H2O-H+=241.1525
Intensity
Counts vs. Mass-to-Charge (m/z)

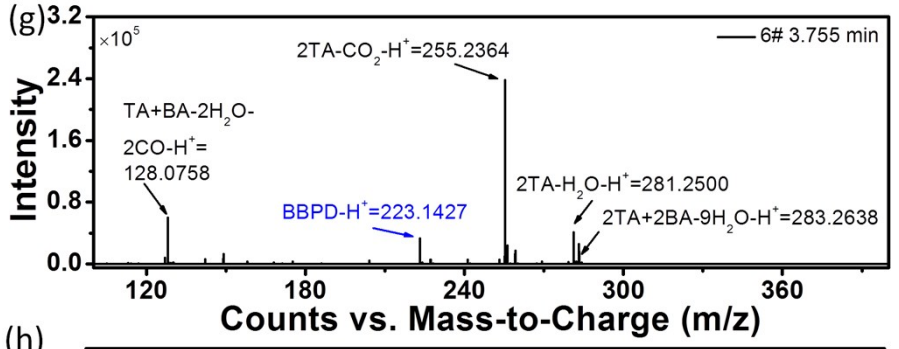
(g)
×10^5
6# 3.755 min
2TA-CO2-H+=255.2364
TA+BA-2H2O-
2CO-H+=
128.0758
BBPD-H+=223.1427
2TA-H2O-H+=281.2500
2TA+2BA-9H2O-H+=283.2638
Intensity
Counts vs. Mass-to-Charge (m/z)

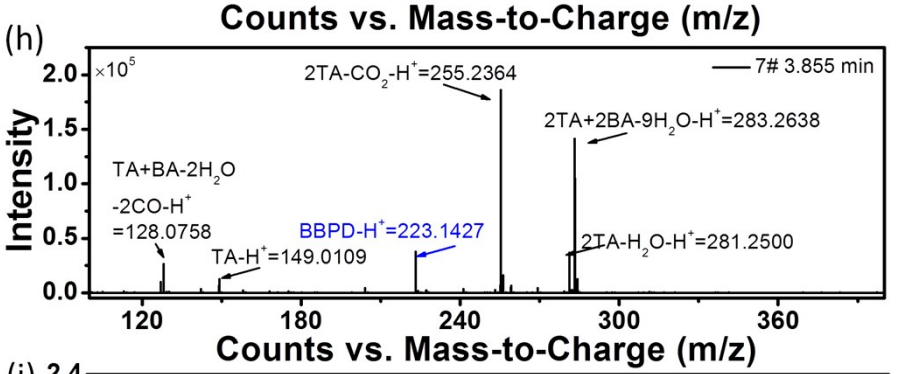
(h)
×10^5
7# 3.855 min
2TA-CO2-H+=255.2364
2TA+2BA-9H2O-H+=283.2638
TA+BA-2H2O
-2CO-H+
=128.0758
BBPD-H+=223.1427
TA-H+=149.0109
2TA-H2O-H+=281.2500
Intensity
Counts vs. Mass-to-Charge (m/z)

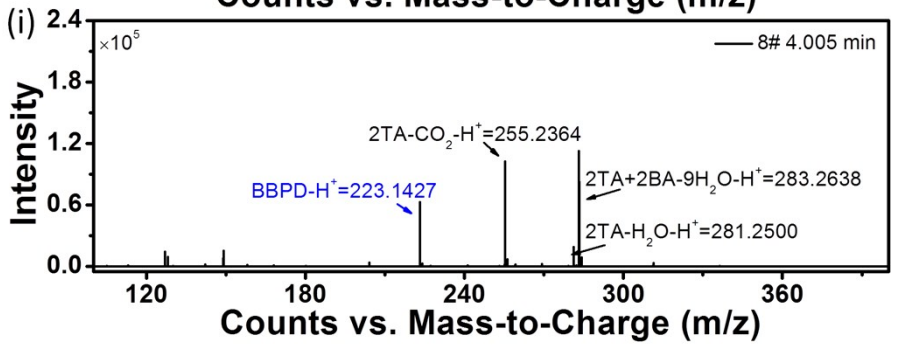
(i)
×10^5
8# 4.005 min
2TA-CO2-H+=255.2364
BBPD-H+=223.1427
2TA+2BA-9H2O-H+=283.2638
2TA-H2O-H+=281.2500
Intensity
Counts vs. Mass-to-Charge (m/z)

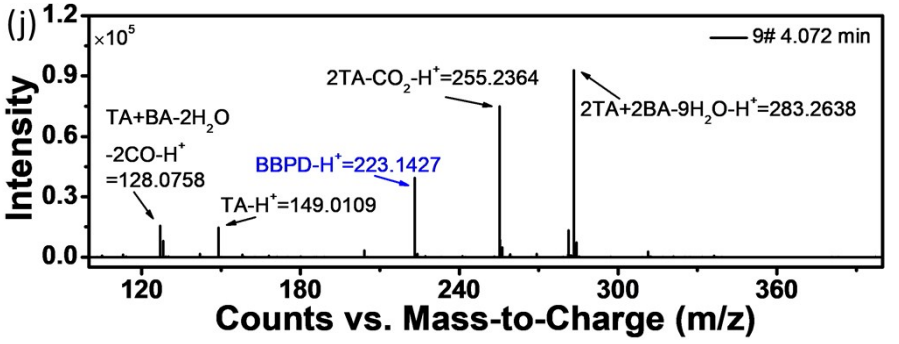
(j)
×10^5
9# 4.072 min
2TA-CO2-H+=255.2364
2TA+2BA-9H2O-H+=283.2638
TA+BA-2H2O
-2CO-H+
=128.0758
BBPD-H+=223.1427
TA-H+=149.0109
Intensity
Counts vs. Mass-to-Charge (m/z)

Figure S7. LC-TOF-MS of GFGA. (a) Chromatograms of GFGA; (b-j) TOF-MS of components 1# to 9# with negative ion mode.

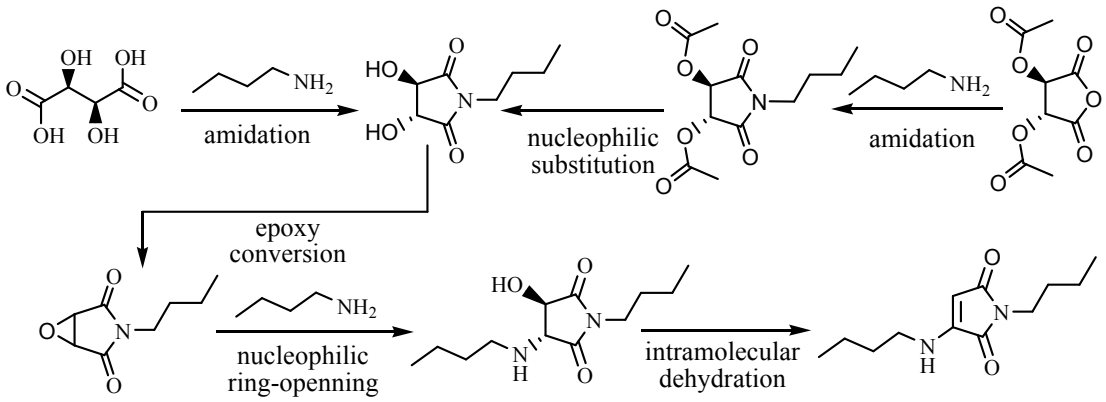

Scheme S1. Illustration of a possible reaction route for the chemical transformation of mono-amine substituted maleimide BBPD.

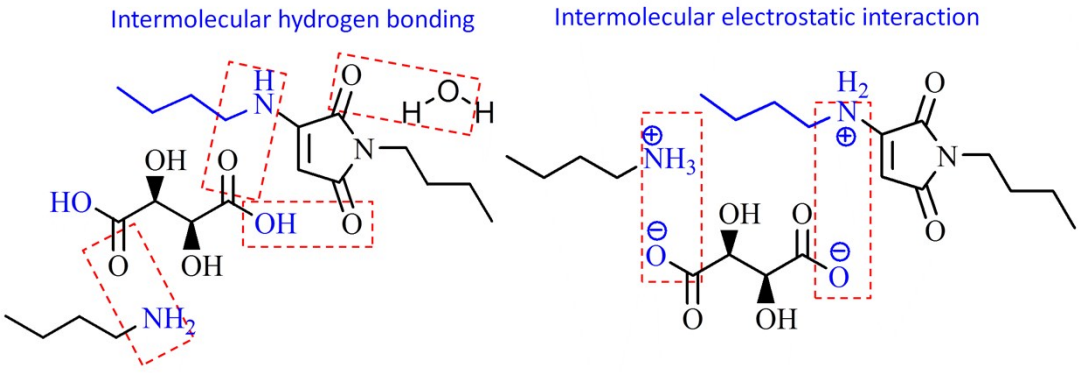

Scheme S2. Proposed intermolecular interactions of the as-prepared GFGA.

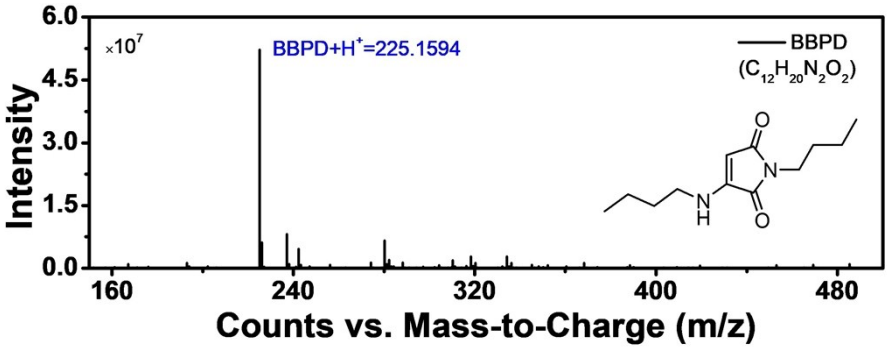

Figure S8. TOF-MS of compound BBPD ($C_{12}H_{20}N_2O_2$) with positive ion mode.

Note: MS signal appeared at 225.1594 is attributed to the characteristic signal of $[M+H]^+$ [$C_{12}H_{20}N_2O_2$ +H^+], which is well matched to the calculated value of 225.1598.

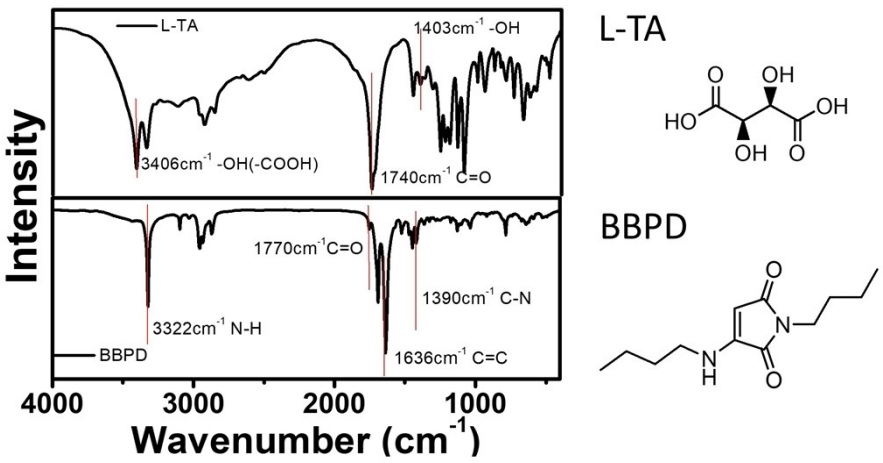

Figure S9. FTIR spectra of L-TA (top) and BBPD (buttom).

Note: The FTIR spectrum of L-TA only displayed -C=O at 1740 cm^{-1}, -OH at 1403 cm^{-1} and -OH in carboxyl group at 3406 cm^{-1}, respectively. The FTIR spectra of BBPD displayed stretching vibration signals of -C=C at 1634 cm^{-1}, -C(O)-N at 1390 cm^{-1}, and -NH at 3322 cm^{-1}, indicating the BBPD was experienced amidation and dihydroxylation processes, which is consistent well with the NMR result.

NMR Spectra

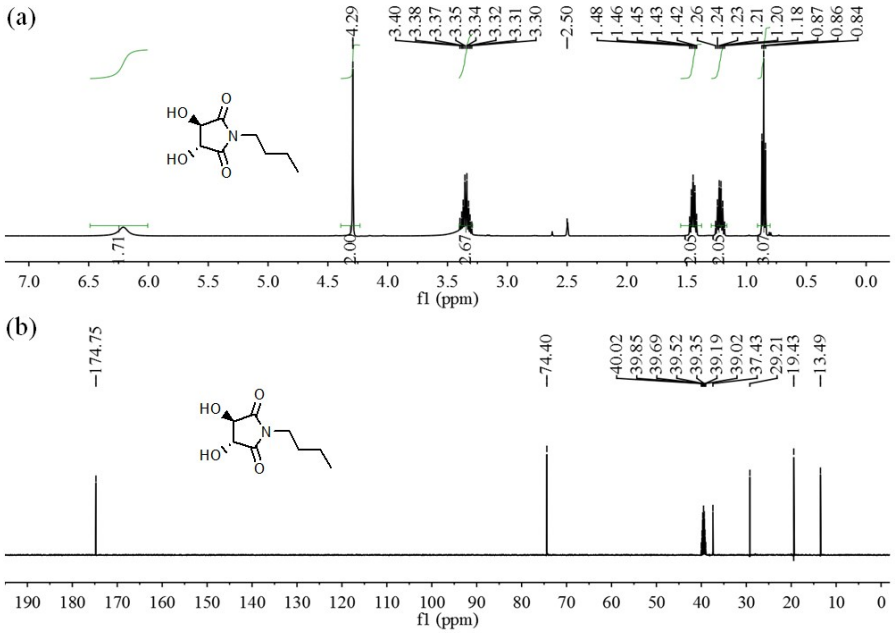

Figure S10. ^{1}H NMR (a) and ^{13}C NMR (b) spectra of BDPD (600MHz, $(CD_3)_2SO$).

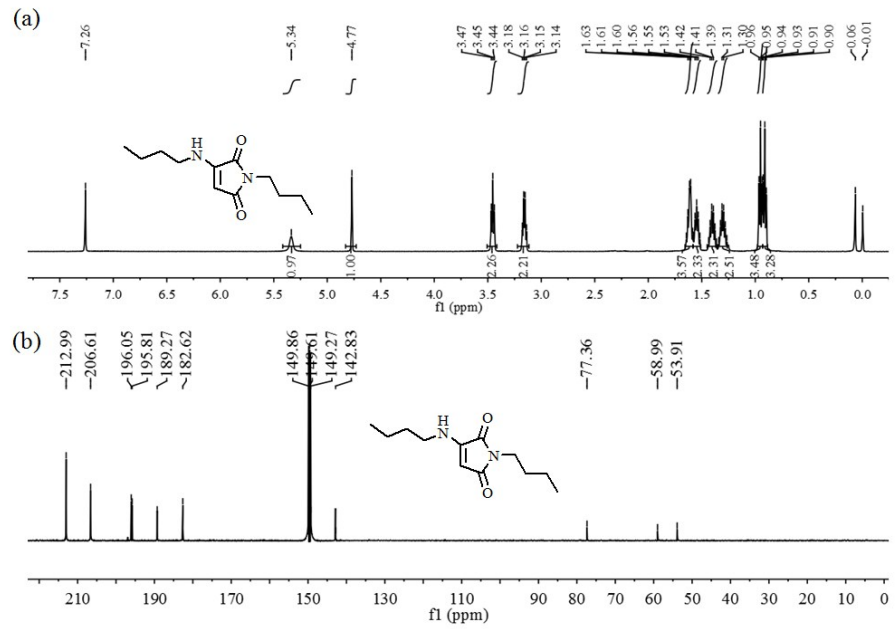

Figure S11. ^{1}H NMR (a) and ^{13}C NMR (b) spectra of BBPD (600MHz, $CDCl_3$).

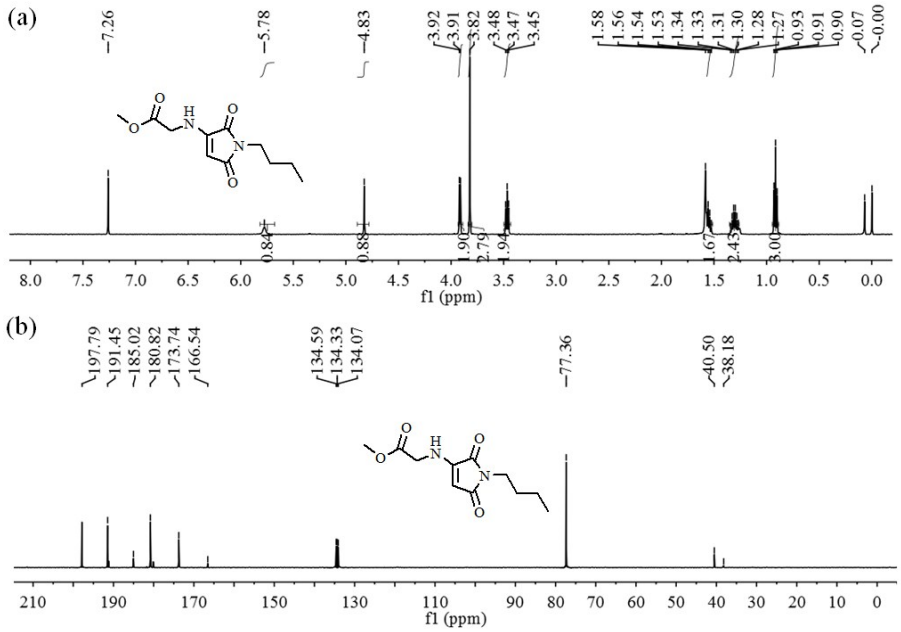

Figure S12. ^{1}H NMR (a) and ^{13}C NMR (b) spectra of BMPD (600MHz, $CDCl_3$).

References

1 M. J. Frisch, G. W. Trucks, H. B. Schlegel, et al, Gaussian, Inc., Wallingford CT, 2016, Gaussian 16, Revision A.03.

2 Y. Xu, M. Wu, Y. Liu, X. Z. Feng, X. B. Yin, X. W. He and Y. K. Zhang, *Chem. Eur. J.* 2013, **19**, 2276; X.-Y. He, B.-Y. Liu, J.-L. Wu, S.-L. Ai, R.-X. Zhuo and S.-X. Chen, *ACS Appl. Mater. Interfaces* 2017, ***9***, 42566.

3 C.-B. Ma, Z.-T. Zhu, H.-X. Wang, X. Huang, X. Zhang, X. Qi, H.-L. Zhang, Y. Zhu, X. Deng, Y. Peng, Y. Han and H. Zhang, *Nanoscale* 2015, **7**, 10162.

4 H.-X. Wang, J. Xiao, Z. Yang, H. Tang, Z.-T. Zhu, M. Zhao, Y. Liu, C. Zhang and H.-L. Zhang, *J. Mater. Chem. A* 2015*,* **3***,* 11287*.*

5 H.-R. Xia, J. Li, W.-T. Sun and L.-M. Peng, *Chem. Commun*. 2014, **50**, 13695.

6 K. Eloh, M. Demurtas, M. G. Mura, A. Deplano, V. Onnis, N. Sasanelli, A. Maxia and P. Caboni, *J. Agr. Food Chem.* 2016, **64**, 4876.

7 L.Robert and V. Pierre, *Helv. Chim. Acta* 2004, **87**, 3167.

8 Y. Marcus, *Chem. Soc. Rev.* 1993*,* **22***, 409.*

9 I. Kunadian, S. M. Lipka, C. R. Swartz, D. Qian and R. Andrews, J. Electrochem. Soc. 2009, **156**, *K110*; Y. Liu, Y.-X. Yu and W.-D. Zhang, J. Phys. Chem. C, 2013, **117**, 12949; F. Meng, J. Li, S. K. Cushing, M. Zhi and N. Wu, J. Am. Chem. Soc. 2013, **135**, 10286.